POLARIZATION OF RADIO WAVES PROPAGATED THROUGH GEORGE VI ICE SHELF

By C. S. M. DOAKE

ABSTRACT. A simplified method of measuring the polarization of radio waves propagated through a glacier was successfully tested on George VI Ice Shelf. An aerial system of three fixed folded dipoles at 45° intervals in a horizontal plane was used to determine the birefringence of the ice, the direction of the effective optic axis and the anisotropy in the reflection coefficient. This system can be used to record polarization data continuously, whether on a sledge or airborne traverse.

PREVIOUS work on the polarization behaviour of radio waves propagated through ice sheets has always been carried out by manually rotated aerials on the ice surface (Jiracek, 1967; Bogorodskiy and others, 1970; Kluga and others, 1973; Bentley, 1975; Hargreaves, 1977; Woodruff and Doake, 1979). Not all workers have appreciated the extent to which the orientation of the transmitting aerial could affect the received signal (Hargreaves, 1977; Doake, 1981), so that the only reported sets of data complete enough to determine accurate polarization parameters are those by Hargreaves (1977), who rotated an aerial system of crossed dipoles, and by Woodruff and Doake (1979), who rotated separate transmitting and receiving aerials. These methods are tedious and cannot be used for continuous data gathering while on a traverse. The work reported here measured polarization parameters using an aerial system of three dipoles, fixed at 45° intervals, in a plane parallel to the ice surface. The theory behind the operation of this method has been explained by Doake (1981). The advantages of the method are that continuous recording is possible, either on the ground or from aircraft, allowing polarization parameters to be mapped over large areas of an ice sheet in the same way as ice thickness.

Aerials were designed for de Havilland Twin Otter aircraft but unfortunately they could not be tested. Instead, the concept was tested using a simplified method at a single site on George VI Ice Shelf in January 1981. On this occasion, normal radio echo-sounding equipment was used, but for continuous recording, two transmitters and three receivers would be required. In addition, provision was made for recording echo strength digitally on a magnetic-cartridge data logger.

Birefringence of ice

Changes in the polarization of radio waves propagated through glaciers have been explained by assuming that ice behaves as an uniaxial birefringent material at frequencies in the VHF band (Hargreaves, 1977; Doake, 1981). The birefringence is assumed to be caused by anisotropy in the permittivity of single-crystal ice. This anisotropy is too small to be detected in laboratory samples (Johari and Charette, 1975) but could be large enough to be significant in ice sheets several hundred metres thick. In a glacier, the overall birefringence would also be controlled by the crystal fabric (Hargreaves, 1978). Because this depends on stress and flow history, measurements of polarization parameters such as birefringence and direction of the effective optic axis should give an insight into the dynamic behaviour of ice sheets. Anisotropy in the reflection coefficient might be related to bedrock lithology and therefore offers a means of gathering subglacial information of geological signifiicance. The flow law for ice is usually taken to be independent of crystal size or orientation; it is suspected, however, that this simplification may not be entirely valid. By mapping the birefringence of ice sheets, it may be possible to deduce when the creation of suitable fabrics becomes important to their flow. There is a related anisotropy in seismic and ultrasonic wave velocities (Bentley, 1975) but data are sparse and difficult to analyse.

Experimental method and results

Three half-wave folded dipoles were fixed to a sledge in the pattern shown in Fig. 1. The radio-echo equipment was mounted on another sledge about 10 m away. The procedure was to record
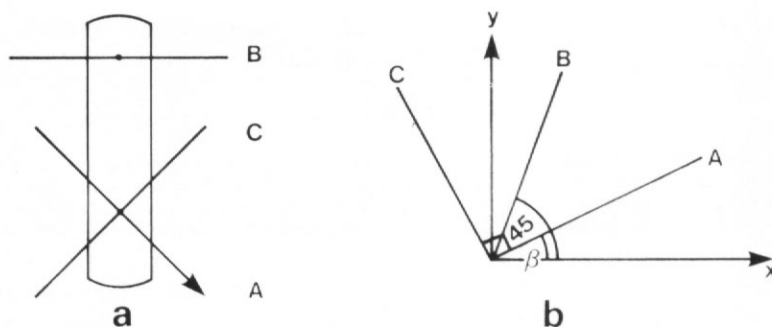
Fig. 1. a. Diagrammatic lay-out of aerials (A, B, C) on the sledge. Each aerial was 2.5 m long; the separation between the centres of B and A,C was 1.76 m. The bearing of A was 200° in the direction indicated by the arrow.
     b. The aerial system is considered to be at an angle β to the coordinate system (x, y).

the echo strength received on each aerial when transmitting on each of the three aerials in turn. Thus, a total of nine values was obtained. The echo strength was determined by increasing the attenuation in the receiver until the echo was reduced to noise level.

The results are shown in Table I. Two complete sets of data were obtained and give an indication of their reproducibility. The first two columns indicate which aerial was used for transmitting and which for receiving. Because the aerials should show reciprocal behaviour for transmitting and receiving (i.e. transmitting on A and receiving on B should give the same result as transmitting on B and receiving on A), the average powers (in dB) shown in column 5 have been calculated taking this into account. The last column identifies the measurements with the nomenclature used to analyse the results.

Theory

Consider the radio waves to propagate vertically through the ice, which is taken to be a simple birefringent material, and to be reflected at normal incidence from a smooth reflector. The direction of the effective optic axis is taken to be the x-axis of the horizontal rectangular coordinate system (x,y), and the aerial system is orientated at an angle β to the x-axis (Fig. 1). The ratio of the reflection coefficients R_x, R_y in the x and y directions is $r = R_x/R_y$ and the total phase shift experienced by the radio waves in their two-way path through the ice is δ. Equations relating the unknown quantities (r, β, δ) to the measured echo strengths are (Doake, 1981):

$$P_1 = P_0 \left(2\cos^4\beta + 2r^2\sin^4\beta + r\sin^2 2\beta \cos\delta\right), \tag{1}$$

$$P_2 = P_0 \left(\cos^2\beta (1 - \sin2\beta) + r^2\sin^2\beta (1 + \sin2\beta) + r\sin2\beta \cos2\beta \cos\delta\right), \tag{2}$$

$$P_3 = P_0 \left(2\cos^2\beta \sin^2\beta (1 + r^2) - r\sin^2 2\beta \cos\delta\right), \tag{3}$$

$$P_5 = P_0 \left(r^2\cos^2\beta (1 + \sin2\beta) + \sin^2\beta (1 - \sin2\beta) - r\sin2\beta \cos2\beta \cos\delta\right), \tag{4}$$

$$P_6 = P_0 \left(2r^2\cos^4\beta + 2\sin^4\beta + r\sin^2 2\beta \cos\delta\right), \tag{5}$$

where P_0 depends on the initial field strength and the reflection coefficients. Table I shows the combination of aerials which corresponds to each measurement of P. Because the airborne system was designed to transmit on only two aerials (corresponding to A and C), the strength measured when transmitting and receiving on B is included only for completeness, while the other two strengths recorded when transmitting on B are used because of the principle of reciprocity of aerials. These extra values are useful for providing an estimate of the accuracy of the echo-strength measurements, which is calculated to be ± 1 dB.

TABLE I. MEASURED ECHO STRENGTHS

Aerials		Echo strength (dB)				
Transmit	Receive	Measured		Average	Normalized	
A	A	38	36	37	0	P_1
A	B	43	41 ⎫			
B	A	42	41 ⎭	42	5	P_2
A	C	41	42 ⎫			
C	A	39	42 ⎭	41	4	P_3
C	B	38	38 ⎫			
B	C	39	40 ⎭	39	2	P_5
C	C	35	35	35	−2	P_6
B	B	49	47			

One solution to Equations (1)–(5) is:

$$\tan 2\beta = \frac{2(P_2 + P_5) - (P_1 + 2P_3 + P_6)}{P_6 - P_1} \tag{6}$$

$$r^2 = [(P_1 + 2P_3 + P_6)\cos2\beta + (P_6 - P_1)]/[(P_1 + 2P_2 + P_6)\cos2\beta - (P_6 - P_1)] \tag{7}$$

$$\cos\delta = [P_1(1 + r^2)\tan^2\beta - P_3(1 + r^2\tan^4\beta)]/[2r\tan^2\beta(P_1 + P_3)]. \tag{8}$$

The form of Equations (6)–(8) shows that, as expected, P_0 does not appear, and also shows that all the measured strengths appear as ratios of each other. This enables one of the measurements to be chosen as a zero reference by subtracting its value (in dB) from the other measurements. Table I shows in column 6 that P_1 has been made zero and the other values normalized accordingly. There are now three unknowns (r, β, δ) and four independent measurements, allowing, in principle, a least-squares solution with an estimate of the accuracy. A possible procedure is given in more detail in the Appendix.

Discussion

A simple solution to Equations (6)–(8), found by substituting values from Table I, is given in the first row of Table II. The error limits have been calculated by allowing the measured values of P to vary one at a time by ± 1 dB and taking the greatest deviations found overall. There is an unresolvable ambiguity of 90° in β, and a corresponding ambiguity in the value of r which would then become $1/r$. This arises because Equations (1)–(5) are unchanged (except for P_0) by substituting ($\beta + 90°$) for β and $1/r$ for r.

TABLE II. COMPUTED VALUES OF THE BIREFRINGENCE PARAMETERS FOR GIVEN VALUES OF POWER P_i

Measured powers (dB)					Solution			
P_1	P_2	P_3	P_5	P_6	r		β	δ
0	5	4	2	−2	0.63	0.21	$-41° \pm 3°$	$126° \, {}^{+\,20°}_{-\,4°}$
0	5	5	3	0	1		$-40°$	$130°$

Allowing for these ambiguities, the results show that the optic axis is aligned at either 69° or 159° and that r is 1.58 or 0.63, respectively. For comparison, the ice-flow direction measured on a nearby stake scheme is 300°. A similar lack of correlation between the optic axis and flow direction on the Bach Ice Shelf (Woodruff and Doake, 1979) was explained by suggesting that the orientation of the optic axis is controlled by the fabric formed when the ice shelf crosses the hinge line and that subsequent rotation causes the misalignment. Only a mapping of the polarization behaviour along an ice-flow line would show whether or not the optic-axis orientation was related to the flow direction. The value of δ, taken with the ice thickness of 320 m, gives a minimum anisotropy in the single crystal of 0.3%. The value found on the Bach Ice Shelf was 0.5% (Woodruff and Doake, 1979), suggesting that a weaker fabric exists at the George VI Ice Shelf site.

It is difficult to understand the significance of the value of r. Although r has been taken to be a measure of the difference in magnitude of the reflection coefficients along and perpendicular to the optic axis, there is no obvious reason why they should differ in a place where normal radio-echo depth sounding indicated a smooth bottom surface. However, any difference in gain between the aerials, if echo-strength values were not corrected accordingly, would affect the value of r. If we assume that the ice-reflection coefficient is isotropic ($r = 1$), then P_1 should equal P_6 (Equations (1) and (5)). The measured 2 dB difference between P_1 and P_6 could then be ascribed to a difference in gain between aerials A and C. Assuming that aerial C has a gain of -1 dB compared with aerials A and B would give the adjusted values for P_1 to P_6 shown in the second row of Table II. When $P_1 = P_6$, an alternative expression for δ to Equation (6) is given by

$$\tan 2\beta = 2P_3/(P_5 - P_2).$$

Using this equation and Equation (8) gives a value for β of $-40°$ and for δ of 130°, agreeing very well with the values previously calculated. Calibration tests carried out on the aerials did not appear to give consistent answers, so no correction was made to the measurements, but the most likely explanation for r not being unity is that there are variations of ≈ 1 dB between aerials rather than there being an anisotropic reflecting surface.

Conclusion

A static three-aerial array has been used to determine polarization parameters of George VI Ice Shelf. The measurements appear to be internally consistent and give sensible results. There is no means of checking their accuracy but reasonable confidence may be placed in their quoted limits. The method seems to be well suited for operating from aircraft, which was the original intention, but care needs to be taken to calibrate the aerials accurately.

REFERENCES

BENTLEY, C. R. 1975. Advances in geophysical exploration of ice sheets and glaciers. *Journal of Glaciology*, **15**, 113–35.

BOGORODSKIY, V., TREPOV, G. V. *and* B. A. FEDEROV. 1970. On measuring dielectric properties of glaciers in the field. (*In* GUDMANSEN, P., *ed. Proceedings of the international meeting on radioglaciology, Lyngby, Denmark*, 20–31.)

CLARK, D. 1963. *Plane and geodetic surveying. Vol. 2. Higher surveying.* London, Constable & Co. Ltd.

DOAKE, C. S. M. 1981. Polarisation of radio waves in ice sheets. *Geophysical Journal of the Royal Astronomical Society*, **64**, 539–58.

HARGREAVES, N. D. 1977. The polarisation of radio signals in the radio echo sounding of ice sheets. *Journal of Physics D: Applied Physics*, **10**, 1285–304.

————. 1978. The radio frequency birefringence of polar ice. *Journal of Glaciology*, **21**, 301–13.

JIRACEK, G. R. 1967. Radio sounding of Antarctic ice. *University of Wisconsin Geophysical and Polar Research Center. Research Report Series*, No. 67-1, 127 pp.

JOHARI, G. P. *and* P. A. CHARETTE. 1975. The permittivity and attenuation in polycrystalline and single-crystal ice Ih at 35 and 60 MHz. *Journal of Glaciology*, **14**, 293–303.

KLUGA, A. M., TREPOV, G. V., FEDEROV, B. A. *and* KHOKHLOV. 1973. Some results of radio echo sounding of Antarctic glaciers in the summer of 1970–71. *Trudȳ Sovetskoy Antarkticheskoy Ekspeditsii,* **61,** 151–63.
WOODRUFF, A. H. W. *and* C. S. M. DOAKE. 1979. Depolarization of radio waves can distinguish between floating and grounded ice sheets. *Journal of Glaciology,* **23,** 223–32.

APPENDIX

Let the general form of Equations (1)–(5) be written as $P_i = P_i(r, \beta, \delta)$.
Then, assuming that the necessary derivatives are continuous, P_i can be expressed using Taylor's expansion as

$$P_i(r, \beta, \delta) = P_i(r_0, \beta_0, \delta_0) + \left[\frac{\partial P_i}{\partial r}\right]_{\beta_0 \delta_0} \delta r + \left[\frac{\partial P_i}{\partial \beta}\right]_{r_0 \delta_0} \delta\beta + \left[\frac{\partial P_i}{\partial \delta}\right]_{r_0 \beta_0} \delta(\delta) + 0\left[\frac{\partial^2 P}{\partial r^2}\right],$$

where $r = r_0 + \delta r$, etc. The values (r_0, β_0, δ_0) are those used to calculate P_i. Denoting the measured echo strength as M_i, and only considering first-order terms, the observation equations may be written

$$\left[\frac{\partial P_i}{\partial r}\right]_{\beta_0 \delta_0} \delta r + \left[\frac{\partial P_i}{\partial \beta}\right]_{r_0 \delta_0} \delta\beta + \left[\frac{\partial P_i}{\partial \delta}\right]_{r_0 \beta_0} \delta(\delta) = M_i - P_i(r_0, \beta_0, \delta_0), \tag{A1}$$

where $(\delta r, \delta\beta\ \delta(\delta))$ are the corrections made to the estimates (r_0, β_0, δ_0). These observation equations are in a standard form and can readily be solved by least-squares methods to give values for $(\delta r, \delta\beta, \delta(\delta))$: writing Equation (A1) in the condensed form

$$m_{i1} x_1 + m_{i2} x_2 + m_{i3} x_3 = c_i,$$

where $m_{i1} = \left[\frac{\partial P_i}{\partial r}\right]_{\beta_0 \delta_0}$; $m_{i2} = \left[\frac{\partial P_i}{\partial \beta}\right]_{r_0 \delta_0}$; $m_{i3} = \left[\frac{\partial P_i}{\partial \delta}\right]_{r_0 \beta_0}$

$$x_1 = \delta r; \qquad x_2 = \delta\beta; \qquad x_3 = \delta(\delta)$$

and $\quad c_i = M_i - P_i$,

then the "normal" equations are given (Clark, 1963) by

$$\sum_i (m_{i1})^2 x_1 + \sum_i (m_{i1} m_{i2}) x_2 + \sum_i (m_{i1} m_{i3}) x_3 = \sum_i m_{i1} c_i$$

$$\sum_i (m_{i2} m_{i1}) x_1 + \sum_i (m_{i2})^2 x_2 + \sum_i (m_{i2} m_{i3}) x_3 = \sum_i m_{i2} c_i$$

$$\sum_i (m_{i3} m_{i1}) x_1 + \sum_i (m_{i3} m_{i2}) x_2 + \sum_i (m_{i3})^2 x_3 = \sum_i m_{i3} c_i$$

or, in matrix form:

$$Ax = b, \tag{A2}$$

where the elements of the matrix A are

$$a_{jk} = \sum_i m_{ij} m_{ik}$$

and the elements of the column vector b are

$$b_j = \sum_i m_{ij} c_i.$$

Values for m_{ij} can be estimated by calculating values for P_i in a small range around r_0 (β_0, δ_0 kept constant) then taking the gradient, and so on. If P_i are normalized by setting $P_1 = 0$, then the derivatives must be normalized as well. The objective is to use estimated values for (r_0, β_0, δ_0) and solve for the corrections $(\delta r, \delta\beta, \delta(\delta))$. The new values of (r, β, δ) are then used to calculate

P_i. The process continues until $\sum\limits_{i} c_i^2$ (the sum of the squares of the residuals) starts to increase, in which case the previous step has calculated a least-squares fit to the measurements.

Initial values for (r_0, β_0, δ_0) were taken from the solution of Equations (6)–(8), and gave $\sum\limits_{i} c_i^2 = 0.93$. Solving Equation (A2) for $(\delta r, \delta\beta, \delta(\delta))$ gave a value for $\sum\limits_{i} c_i^2$ of 3.53. This implies that the original values were better. Confirmation that the method was working correctly was given by reversing the procedure, i.e. starting with the values $(r_0 + \delta r)$, etc., and observing that the new solution gave a lower value for $\sum\limits_{i} c_i^2$.

An arithmetically simpler alternative is to find best-fit values for r, β and δ separately. The equations to solve in this case are

$$x_j = (\sum\limits_{i} m_{ij}\, c_i)/\sum\limits_{i} (m_{ij})^2,$$

using the same nomenclature as before. (This is equivalent to considering only the diagonal terms in the matrix A in Equation (A2).) A value of $\sum\limits_{i} c_i^2$ of 0.73, slightly lower than the original figure, was obtained by the values $r = 0.665$, $\beta = -40.75°$, $\delta = 126.7°$, which do not differ significantly from the original estimates in Table II.